Global and Planetary Change 240 (2024) 104522

Contents lists available at ScienceDirect

Global and Planetary Change

journal homepage: www.elsevier.com/locate/gloplacha

Shallow-water redox evolution from the Ediacaran to the early Cambrian: Linkages to the early animal innovations

Guang-Yi Wei [a,1], Da Li [b,1], Zunli Lu [c,*], Ganqing Jiang [d], Hong-Fei Ling [a]

[a] State Key Laboratory for Mineral Deposits Research, School of Earth Sciences and Engineering and Frontiers Science Center for Critical Earth Material Cycling, Nanjing University, 163 Xianlin Avenue, Nanjing 210023, China
[b] School of Marine Science and Engineering, Nanjing Normal University, Nanjing 210023, China
[c] Department of Earth Sciences, Syracuse University, Syracuse, NY 13244, USA
[d] Department of Geoscience, University of Nevada, Las Vegas, NV 89154-4010, USA

ARTICLE INFO

Editor: Dr. Maoyan Zhu

Keywords:
Shallow ocean redox
I/(Ca + Mg)
Ce anomaly
South China
Early animals

ABSTRACT

The oceanic oxygenation from the Ediacaran to the early Cambrian (ca. 635–520 Ma) has been commonly linked with the radiation or innovation of early metazoans. However, in this period, the spatio-temporal changes in redox states have not been well constrained for shallow seawater that is proposed to be potential habitats for most metazoans. Here, we report new iodine (I) concentration and Cerium anomaly (Ce/Ce*) data from two Ediacaran–Cambrian carbonate successions in South China. Combined with published data, the new database provides more insights into the evolution of shallow-water redox states on the continental margin. Overall low I/(Ca + Mg) (0.07–1.092 μmol/mol) and high Ce/Ce* (0.64–0.91) indicate frequent presence of low oxygen waters on the Yangtze margin in the early-middle Ediacaran (ca. 635–575 Ma). The initial increases of shallow-water oxygen levels occur from the middle Ediacaran (< ca. 575 Ma), coincident with the rise of the Ediacara biota. However, large variabilities of I/(Ca + Mg) (0.003–4.53) and Ce/Ce* (0.1–0.92) through different sections from the late Ediacaran to the early Cambrian (ca. 575–520 Ma) suggest highly dynamic redox states on both spatial and temporal scales before the Cambrian explosion in a narrow sense. The new I/(Ca + Mg) and Ce/Ce* data bolster the case that the Ediacaran–Cambrian oceans have much lower oxygenation levels than recent fully oxygenated oceans, and frequent redox fluctuations in habitats may have stimulated the early animal innovations.

1. Introduction

The Ediacaran and Cambrian periods produced fossil records of the earliest metazoans and the establishment of the Cambrian Evolutionary Fauna in oceans (Marshall, 2006; Xiao and Laflamme, 2009; Erwin et al., 2011; Darroch et al., 2018). The reshaping redox landscape on Earth's surface has been considered as one of the most critical factors impacting the earliest animal radiations (Zhang et al., 2014; Wood et al., 2019; Cole et al., 2020). The classical view highlights progressive increases in atmospheric-oceanic oxygenation level from the late Neoproterozoic, closely linked to the rise of metazoans (e.g., Och and Shields-Zhou, 2012; Lyons et al., 2014; Sperling et al., 2013; Tostevin and Mills, 2020). However, recent studies have suggested that the overall extent of global oceanic oxygenation was limited during the Ediacaran and Cambrian periods (Sperling et al., 2015b; Stolper and Keller, 2018; Wei et al., 2021a), and the physiological thresholds of oxygen for early metazoans may have been lower than modern animals (Mills et al., 2014; Sperling et al., 2015a). Thus, there are still intense debates about the role of redox changes in triggering the radiation of metazoans (Butterfield, 2009; Lenton et al., 2014; Wood et al., 2019; Cole et al., 2020). Moreover, given that early metazoans from the Ediacaran to the Cambrian appear to have originated in the shallow-marine settings of the continental shelf rather than deep or pelagic ocean (Tarhan et al., 2018; Servais and Harper, 2018; Wood et al., 2019), more (semi-) quantitative constraints on shallow-water redox states may provide critical insights into the role of oceanic oxygenation on the rise of metazoans and the expansion of ecological structure (Reinhard et al., 2016; Cole et al., 2020). So far, most studies concentrate on the redox

* Corresponding author.
E-mail addresses: guangyiwei@nju.edu.cn (G.-Y. Wei), lida@njnu.edu.cn (D. Li), zunlilu@syr.edu (Z. Lu).
[1] These authors contributed equally to this work.

https://doi.org/10.1016/j.gloplacha.2024.104522
Received 17 December 2023; Received in revised form 5 July 2024; Accepted 17 July 2024
Available online 18 July 2024

landscape of global ocean or regional bottom seawater from the Ediacaran to the early Cambrian (see reviews in Wei et al., 2021b; Tostevin and Mills, 2020). The secular changes in shallow or upper water redox states have not been adequately evaluated throughout this important time interval.

In this study, we analyze and compile iodine and cerium anomaly data [presented as I/(Ca + Mg) and Ce/Ce*] in carbonate successions on the Yangtze margin (Fig. 1), aiming to better evaluate the temporal evolution of shallow-water redox from the Ediacaran to the early Cambrian and the spatial redox dynamic across the transection of continental margins. We suggest that paired investigations of I/(Ca + Mg) and Ce/Ce* can provide useful information about shallow-water redox states. Finally, we argue that increases in oxygenation level of shallow seawater occurred from the middle–late Ediacaran (perhaps at the onset of 'Shuram-Wonoka Excursion', < ca. 575 Ma) followed by large swings through time. Well-oxygenated shallow water habitats were much less ubiquitous across the Ediacaran and Cambrian compared to modern oceans.

2. Background of I/(Ca + Mg) ratio and Ce anomaly as shallow-marine redox proxies

Carbonate associated iodine, reported as I/(Ca + Mg) ratios in limestones and dolostones, is a proxy for upper ocean redox states (see recent review in Lu et al., 2020). It has been applied in ancient and recent geologic time (e.g., Lu et al., 2010, 2016; Zhou et al., 2014; Hardisty et al., 2014, 2017; Lu et al., 2018; Wei et al., 2019; Shang et al., 2019). For dissolved iodine anion in the modern ocean, it has a long residence time of ~300 kyr and a relatively uniform concentration of 0.45 μmol/L (Broecker and Peng, 1982). The thermodynamically stable forms of iodine in seawater are iodate (IO_3^-) and iodide (I^-), whose species are determined by seawater oxygen level (Wong, 1991). The IO_3^- is converted to I^- in low oxygen waters (Rue et al., 1997; Hardisty et al., 2021); accordingly, IO_3^- concentrations are positively correlated to dissolved O_2 concentrations above oxygen-minimum zones (OMZs) (Fig. 2A).Since IO_3^- is the only chemical form of iodine that is incorporated into the structure of carbonate (Lu et al., 2010; Kerisit et al., 2018), I/(Ca + Mg) ratios of calcium carbonate will decrease when dissolved O_2 of the ambient seawater declines to trigger IO_3^- reduction. The I/(Ca + Mg) signal of shallow-water carbonates is an effective tracer for hypoxic or suboxic conditions related to the presence of OMZs or fluctuations in depth of oxycline (Lu et al., 2016, 2020). It should be noted that the oxidation rate of I^- is kinetically slower than reduction of IO_3^-; thus, IO_3^- and I^- can coexist in oxygenated modern seawater and the I/(Ca + Mg) ratios of carbonates can also be influenced by regional mixing of adjacent water masses (Lu et al., 2020; Hardisty et al., 2017, 2021). In ancient oceans at relatively low oxygen levels, the dissolved O_2 concentrations act as a first-order control on I/(Ca + Mg) ratios of marine carbonates. Taken together, several semi-quantitative estimations of shallow-water O_2 level have been provided for I/(Ca + Mg) proxy based on observations in recent oceans.

Compared to other rare earth elements (REEs), Ce has unique redox chemistry and its valence states are sensitive to oxidation level. Under oxic conditions, the dissolved Ce^{3+} can be oxidized to insoluble Ce^{4+} and then precipitate from the water column as discrete Ce oxides or absorption onto the surface of Mn (IV)-(oxyhydr)oxide particles and other particulate matter (Sholkovitz and Shen, 1995; Byrne and Kim, 1990). Accordingly, the oxygenated waters would be depleted in Ce relative to other REEs. Such depletion is expressed as negative "Ce anomaly" (Ce/Ce*), which is newly defined by:

$$Ce \Big/ Ce^{*} = \frac{[Ce]_{SN}}{\left([Pr]_{SN}\right)^{2} \Big/ [Nd]_{SN}}$$

where SN denotes the shale-normalized value of each element (Lawrence et al., 2006). This equation can exclude pseudo negative Ce anomaly resulting from overabundance of La in aquatic systems (Lawrence et al., 2006). Although discrete Ce oxides can form in the water column, oxidation of Ce^{3+} generally occurs on the surface of metal oxide particles (Sholkovitz and Shen, 1995), resulting in a positive Ce anomaly (Ce/Ce* > 1.2) in these oxides and a negative Ce anomaly (Ce/Ce* < 0.8) in the water column (Tostevin, 2021). The scavenging of Ce in oxic waters is dominated by formation of metal oxides (e.g., Mn (IV)-(oxyhydr)oxide particle), supported by the nadir of seawater Ce/Ce* across the peak of Mn (IV) particles (Ling et al., 2013). Accordingly, the occurrence of positive or negative Ce anomaly in the water column is closely linked to marine Mn cycle (i.e., oxidation and reduction of Mn (IV)-(oxyhydr)oxides) and the depth of seawater redox chemocline, instead of the vertical dissolved O_2 concentrations (Fig. 2). In this view, significantly negative Ce anomalies generally develop at the water depth with substantial particle Mn formation, rather than high dissolved O_2 concentrations in ambient seawater (Fig. 2, Ling et al., 2013). Hence, preservation of seawater negative Ce anomaly likely reflects the dissolved O_2 concentrations of shallow seawater higher than ~10 μM that is considered as a threshold value for Mn (IV) reduction (Tostevin et al., 2016). Meanwhile, a positive Ce anomaly or the absence of Ce anomaly may provide evidence for suboxic conditions but not necessarily indicate fully anoxic conditions (Ling et al., 2013; Tostevin, 2021).

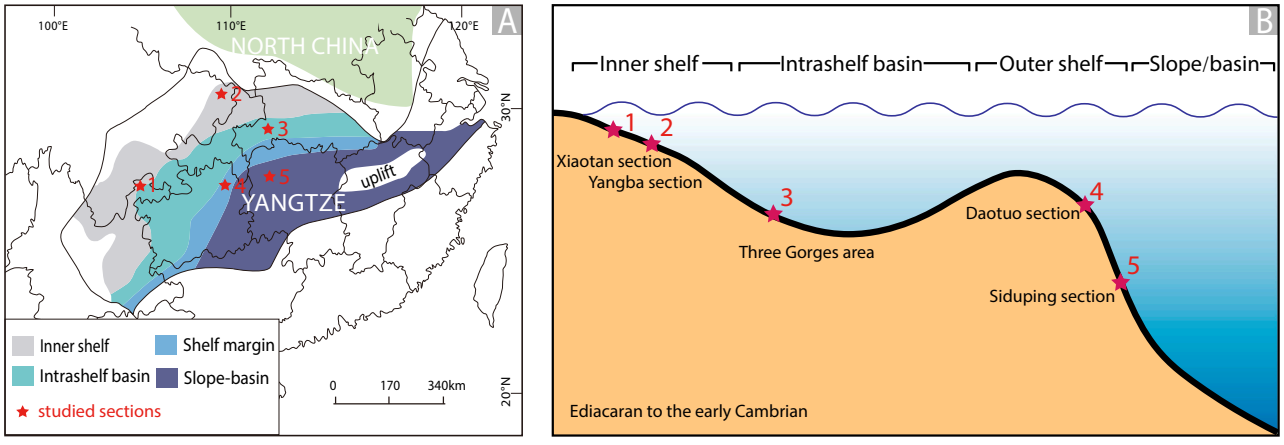

Fig. 1. (A) Geological map of South China with locations of the studied sections and (B) reconstruction of the shelf-to-basin paleogeographic transect on the Yangtze margin during the late Ediacaran (modified from Jiang et al., 2011).

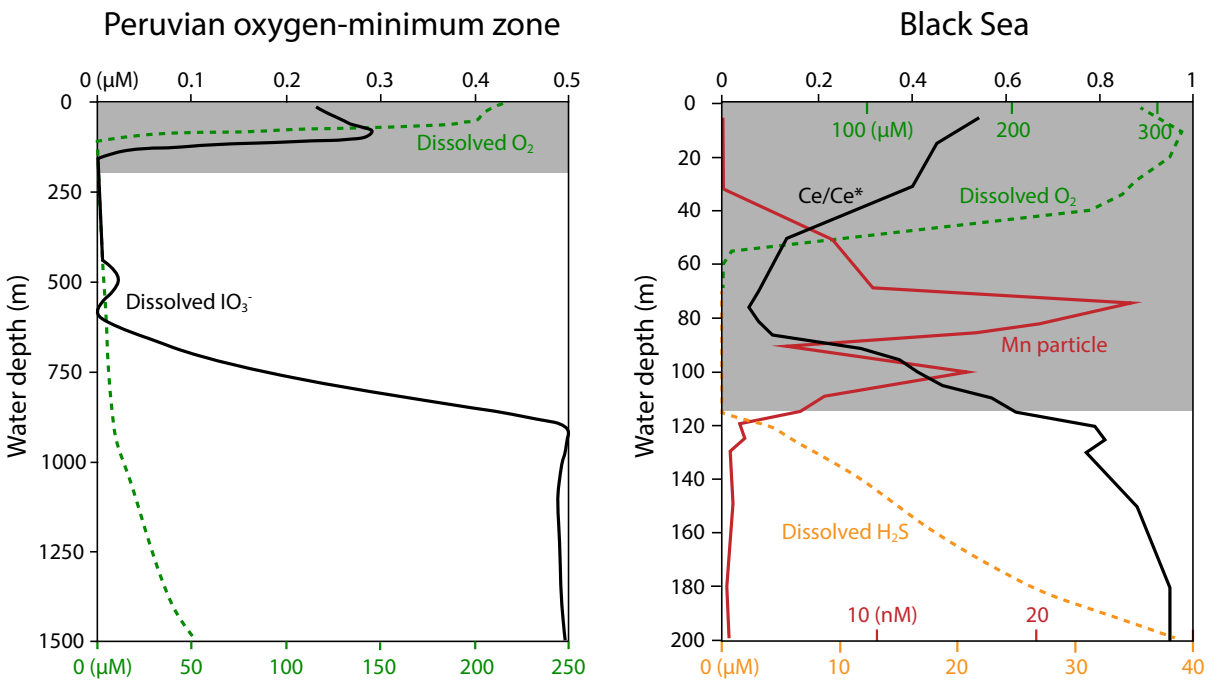

Fig. 2. Depth profiles of (A) dissolved iodate (IO_3^-) and O_2 in the Peruvian oxygen-minimum zone and (B) Ce anomaly (Ce/Ce*), dissolved O_2 and H_2S and Mn (IV) particle in the Black Sea (modified after Ling et al., 2013 and Hardisty et al., 2017). The grey zones in (A) and (B) denote the redox transitions in shallow seawater.

3. Materials and methods

3.1. The studied sections

We collected carbonate samples from two Ediacaran–Cambrian shallow marine carbonate-dominated sections (Jiulongwan–Gaojiaxi–Yanjiahe section and Xiaotan section) in South China that have been previously studied for C-, O-, Ca-, Sr-, U-isotopes (Ling et al., 2013; Li et al., 2013; Wei et al., 2018, 2021b, 2022a, 2022b) (Fig. 1). The time and correlation of these sections are calibrated by integrating biostratigraphy, C isotope chemostratigraphy and radio-isotopic dates. These two sections together provide a continuous Ediacaran to early Cambrian sedimentary record (ca. 635–525 Ma) (Yang et al., 2021; Bowyer et al., 2022).

The Jiulongwan–Gaojiaxi–Yanjiahe section in the Yangtze Gorges area, Hubei Province, China records an intrashelf basin paleoenvironment (subtidal shale-carbonate facies) from the Ediacaran to the early Cambrian (Jiang et al., 2011). In the Jiulongwan section, the Doushantuo Formation can be divided into four lithostratigraphic members. Member I is a ~ 5 m thick post-Marinoan cap carbonate overlying the glacial diamictite of the Nantuo Formation, with a Zircon U—Pb age of 635.2 ± 0.6 Ma in the upper part (Condon et al., 2005). Member II consists of ~70 m alternating black shale and dolostone beds with pea-sized cherty nodules, in which complex microfossils (acanthomorphic acritarchs, animal embryos, multicellular algae, filamentous and coccoidal cyanobacteria) (e.g., McFadden et al., 2008). Member III is ~50 m thick and consists of dolostone beds intercalated with cherty layers in the lower part and interbedded with limestone beds in the upper part. This member is characterized by significantly negative C isotope values, which have been correlated to the "Shuram–Wonaka Excursion" in the middle Ediacaran (McFadden et al., 2008; Rooney et al., 2020). Member IV is a ~ 10 m thick black shale interval (i.e., "Miaohe Member" in the Yangtze Gorges area). In the Gaojiaxi–Yanjiahe section, the Dengying Formation documents the upper Ediacaran carbonate succession (< ~551 Ma) (Condon et al., 2005). It can be divided into three members described as, from the base to top, the 1) Hamajing Member: intraclastic and oolitic dolomitic grainstone; 2) Shibantan Member: dark grey laminated micritic limestone, with cherty laminae in the upper part; and 3) Baimatuo Member: micritic and finely crystalline dolostone. Overlying the Dengying Formation is the Yanjiahe Formation, which spans the Ediacaran-Cambrian boundary.

The Xiaotan section, NE Yunnan Province, China records an inner shelf paleoenvironment (peritidal carbonate-dominated facies) from the late Ediacaran to the Cambrian (Li et al., 2013). The Xiaotan section comprises, from base to top, the upper Ediacaran Dengying Formation and lower Cambrian Zhujiaqing, Shiyantou, Yu'anshan, Hongjingshao and Wulongqing formations. The Dengying Formation in the Xiaotan section can be divided into three members from the base to top: 1) the Donglongtan Member (~35 m thick), consisting of laminated dolostone; 2) the Jiucheng Member, consisting of poorly outcropping shale; and 3) the Baiyanshao Member (~75 m thick), containing thickly bedded to massive, grey to dark grey, finely crystalline dolostone. The Dengying Formation is overlain by the Cambrian Zhujiaqiang Formation, comprising three members, from base to top: 1) the Daibu Member (~30 m thick), consisting of interbedded dark, dolomitic chert and pale yellowish siliceous dolostone of thin to intermediate thickness; 2) the Zhongyicun Member (~75 m thick), consisting of a thick phosphorite layer interbedded with laminated dolostones, and containing the lowest Cambrian *Anabarites trisulcatus-Protohertzina anabarica* and *Siphogonuchites triangularis-Paragloborilus subglobosus* small shelly fossil assemblages (Li and Xiao, 2004); and 3) the Dahai Member (~65 m thick), consisting of pale grey, thickly bedded fossiliferous limestone containing the *Heraultipegma yunnanensis* small shelly fossil assemblage (Li and Xiao, 2004).

3.2. Measurements of I/(Mg + Ca) and Ce/Ce*

The carbonate samples, including limestones and dolostones, in the Jiulongwan–Gaojiaxi–Yanjiahe section and Xiaotan section were selected and leached with weak acids for analyses of I/(Ca + Mg) and Ce anomaly. Approximately 35 mg of powder was weighed out on a microgram balance and then thoroughly rinsed with de-ionized water. The 3% nitric acid were added to the cleaned samples for dissolution. The solution was then diluted to ~50 ppm Ca, assuming samples

containing 100% $CaCO_3$. Iodine calibration standards were freshly prepared from potassium iodate powder. To stabilize iodine, 0.1% tertiary amine solution was added soon after the sample dissolution, followed by ICP-MS measurements immediately. The sensitivity of iodine was tuned to above 80 kcps for a 1 ppb standard. The precision for ^{127}I is typically better than 1%. The long-term accuracy is guaranteed by frequently repeated analyses of the reference material JCp-1 (Lu et al., 2010). The detection limit of I/(Ca + Mg) is generally better than 0.1 μmol/mol. Mg concentrations were calibrated by a Merck multi-element standard. All of the measurements were performed using a quadrupole ICP-MS (Bruker M90) at Syracuse University.

For other major and trace elemental (including REEs) analyses, the sample powders were leached using 1 N acetic acid to dissolve the carbonate component partially and avoid REEs released from the silicate detrital materials. Trace and major elemental concentrations of solution were measured on an Agilent 7900 Quadrupole ICP–MS with RSD <5%, based on repeated analyses of the rock standard JDo-1 and OSIL Atlantic seawater at Nanjing University. The REEs contents of the studied samples are normalized with the values of post-Archean Australian shale (PAAS) (Pourmand et al., 2012), and Ce/Ce* values are calculated using the equation from Lawrence et al. (2006).

4. Results and discussion

Previous studies have conducted biostratigraphic and C isotope chemostratigraphic investigations, which we use to constrain the timing correlations of the sections in this study (McFadden et al., 2008; Ling et al., 2013; Li et al., 2013; Yang et al., 2021; Bowyer et al., 2022). This study reports new I/(Ca + Mg) and Ce/Ce* data of the bulk carbonates, together with compilations of published Ce/Ce* data from the same batch of samples in these sections (Ling et al., 2013; Wei et al., 2018, 2020), which are presented in Supplemental table and Fig. 3. In the Jiulongwan section of the Yangtze Gorges area, carbonates from the Doushantuo Formation show I/(Ca + Mg) ratios from 0.07 μmol/mol to 1.09 μmol/mol, and Ce/Ce* from 0.64 to 0.91. In the Gaojiaxi-Yanjiahe section, carbonates from the Dengying Formation have uniformly low I/(Ca + Mg) ratios from 0.12 μmol/mol to 0.25 μmol/mol, and Ce/Ce* from 0.30 to 0.92. In the Xiaotan section, carbonates from the Dengying Formation have I/(Ca + Mg) ratios higher than those in the Gaojiaxi-Yanjiahe section, ranging from 0.18 μmol/mol to 2.39 μmol/mol. The Ce/Ce* values of the Dengying Formation range from 0.48 to 0.90. Carbonates from the Zhujiaqing Formation show I/(Ca + Mg) ratios from 0.04 to 5.09 with a nadir in the Dahai Member. The Ce/Ce* values of the Zhujiaqing Formation range from 0.40 to 0.81.

4.1. Effects of silicate detrital contamination and diagenetic alteration

The terrestrial detrital aluminosilicates in bulk carbonates commonly have much higher REEs contents than pure carbonate minerals and their dissolution during the digestion of samples may affect the REEs patterns and Ce/Ce* values of the marine carbonates (Ling et al., 2013; Tostevin, 2021). For REEs analyses, a weak acid (1 N acetic acid) is used to dissolve the samples. This sequential leaching method would have effectively reduced the detrital contamination. Moreover, we use following criteria: Al < 0.35%, Th < 0.5 ppm, Sc < 2 ppm and ∑REEs <12 ppm in acetic acid leached carbonate solutions to target samples that preserve primary seawater Ce/Ce* signature (Ling et al., 2013). Taken together, we indicate that the screened I/(Ca + Mg) and Ce/Ce* data in this study are not significantly influenced by terrestrial detrital contamination.

Previous studies have suggested that carbonate diagenesis can affect I/(Ca + Mg) ratios of marine carbonate, during which carbonate-associated IO_3^- is reduced to I^- and released from the carbonate minerals (Lu et al., 2010; Hardisty et al., 2017). The dolomitization and neomorphism of primary carbonate minerals will significantly decrease the I/(Ca + Mg) ratios of the diagenetic carbonates, especially when diagenesis occurs in O_2-depleted pore-water (Hardisty et al., 2017). In modern Great Bahama Bank, both meteoric and marine burial

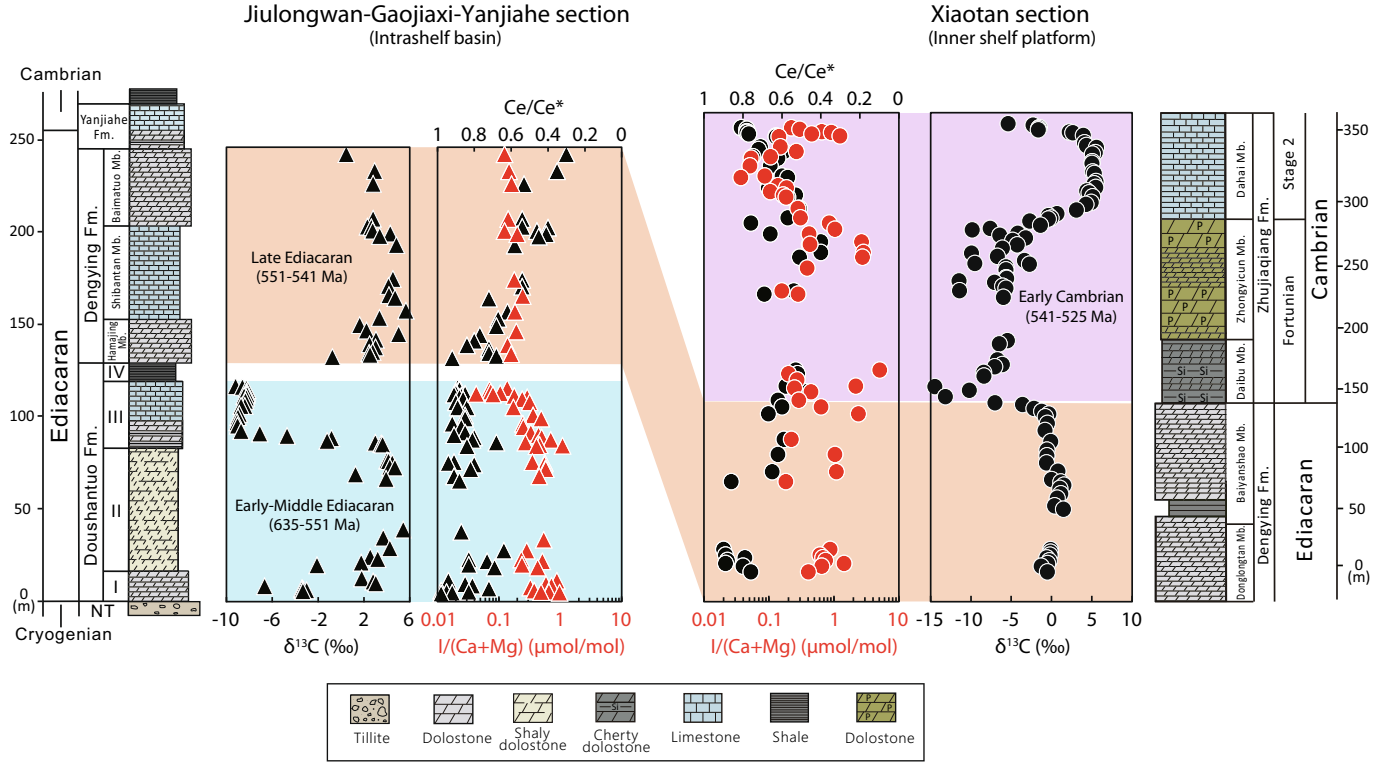

Fig. 3. Stratigraphic columns and geochemical profiles of $\delta^{13}C$, Ce/Ce* and I/(Ca + Mg) data from the Jiulongwan-Gaojiaxi-Yanjiahe section (Yangtze Gorges area) and the Xiaotan section (NE Yunnan).

diagenetic carbonates exhibit lower I/(Ca + Mg) ratios relative to primary carbonates (Hardisty et al., 2017). The REEs in carbonates are generally not susceptible to early diagenesis, likely due to their high partition coefficients between carbonate minerals and seawater (Webb et al., 2009). Studies of modern carbonate platform also suggest that the primary REEs signals can be well preserved in both meteoric and marine burial diagenetic carbonates (e.g., Great Bahama Bank, Liu et al., 2019). Previous studies commonly use relationships between $\delta^{18}O$, Mn/Sr, Mg/Ca and I/(Ca + Mg) to detect the potential effects of diagenetic alteration. However, based on data from the Great Bahama Bank (Hardisty et al., 2017; Liu et al., 2019), decreased I/(Ca + Mg) can be observed in low-Mg calcites that experience both marine and meteoric diagenesis. Using Ca isotopes and Sr contents, previous studies have investigated the carbonate mineralogy and early diagenesis of the studied sections (Wei et al., 2022a, 2022b). In general, marine burial diagenesis, including dolomitization, results in the co-varying $\delta^{44}Ca$ values and Sr contents of marine carbonates (increasing $\delta^{44}Ca$ and decreasing Sr content), which is related to diagenetic extents and regimes (Higgins et al., 2018; Ahm et al., 2018). We further compare I/(Ca + Mg) and Ce/Ce* values with $\delta^{44}Ca$ values and Sr contents to evaluate the potential effects of carbonate diagenesis on I/(Ca + Mg) and Ce/Ce* values (Fig. 4). Lack of appreciable covariations among them suggests that changes in I/(Ca + Mg) and Ce/Ce* values are not in coincidence with $\delta^{44}Ca$ and Sr content, thus not controlled by diagenetic alteration. Potential diagenetic alterations in each interval are further examined in the following discussions.

4.2. Spatial and temporal patterns in shallow-water redox the Yangtze margin

4.2.1. The Doushantuo Formation in South China (ca. 635–551 Ma)

Carbonates from the Doushantuo Formation in the Jiulongwan section overall show low I/(Ca + Mg) ratios (0.41 ± 0.24, 1σ), ranging from 0.04 to 1.09. Such low values may indicate low oxygenation levels of shallow seawater on the Yangtze margin, similar to those of Proterozoic seawater baseline (I/(Ca + Mg) = ~0.5 μmol/mol, Hardisty et al., 2014, 2017). Carbonate diagenesis, especially dolomitization can also contribute to lowering I/(Ca + Mg) ratios of ancient carbonates (e.g., He et al., 2020), considering that most of the carbonates deposited from the Jiulongwan section are marked by fluid-buffered conditions based on Ca isotope records (Wei et al., 2022a, 2022b). Given that deeper sections are more likely dominated by sediment-buffered conditions (e.g., Higgins et al., 2018; Busch et al., 2022; Wei et al., 2022b), we further compile I/(Ca + Mg) ratios of carbonates from different facies in the Yangtze area, including the Daotuo section (outer shelf) and Siduping section (slope) (data from Hardisty et al., 2017; Wei et al., 2019). All these sections show low I/(Ca + Mg) ratios (< 0.5 μmol/mol on average) in the lower and middle Doushantuo Formation before the DOUNCE (Doushantuo negative carbon isotope excursion) event in South China (i.e., 'Shuram-Wonoka excursion', Rooney et al., 2020) (Fig. 5). Although the diagenetic effects on I/(Ca + Mg) ratios of the carbonates cannot be excluded, uniformly low carbonate I/(Ca + Mg) ratios in different sections (intrashelf basin–outer shelf–slope facies) can partly provide evidence for low oxygenation levels of shallow seawater on the Yangtze margin during the early–middle Ediacaran (ca. 635–575 Ma). This

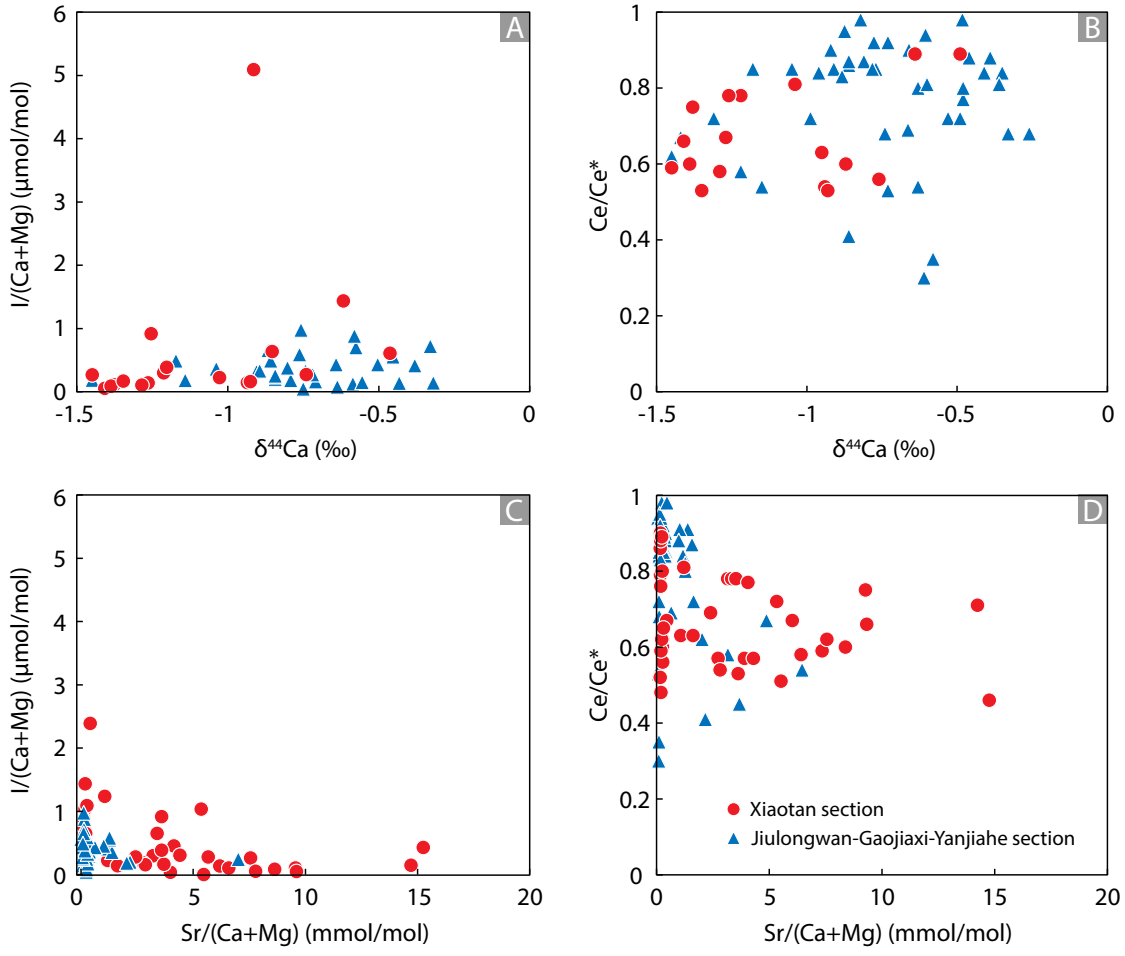

Fig. 4. Cross-plots of (A) I/(Ca + Mg) vs. $\delta^{44}Ca$, (B) Ce/Ce* vs. $\delta^{44}Ca$, (C) I/(Ca + Mg) vs. Sr/(Ca + Mg) and (D) Ce/Ce* vs. Sr/(Ca + Mg). The $\delta^{44}Ca$ data are from Wei et al. (2022a, 2022b).

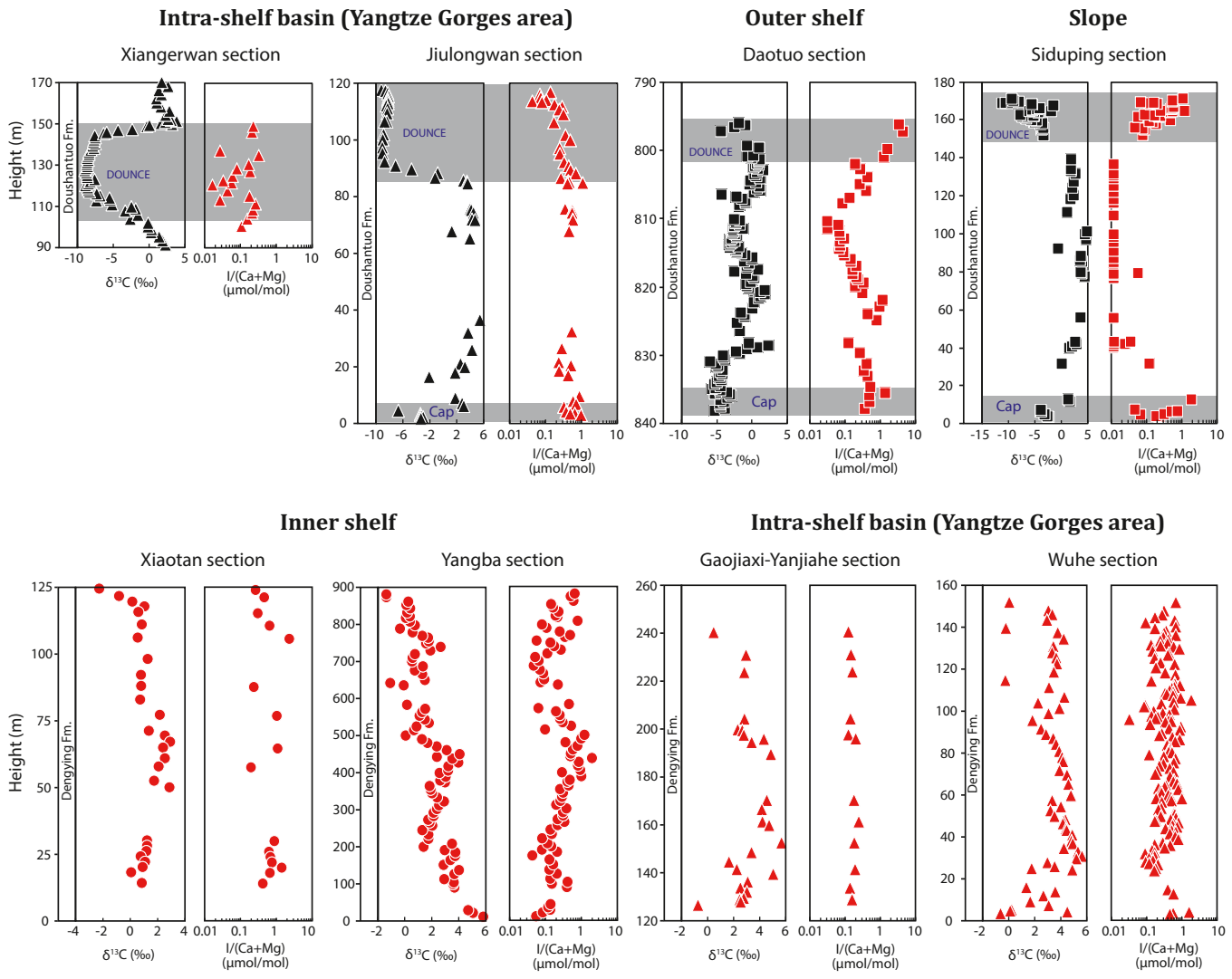

Fig. 5. Correlations of $\delta^{13}C$ and I/(Ca + Mg) data in the Doushantuo carbonates from different paleogeographic locations on the Yangtze margin. The data of the Xiangerwan and Daotuo sections are from Wei et al. (2019) and the Siduping section are from Hardisty et al. (2017).

observation is also supported by lack of significantly negative Ce anomalies in these carbonates that are considered being less sensitive to diagenetic alterations (Fig. 3) (Ling et al., 2013; Wei et al., 2018).

During the interval of 'Shuram-Wonoka excursion" in South China (< 575 Ma), carbonates in different facies exhibit heterogeneous I/(Ca + Mg) ratios (Fig. 5). The Xiangerwan and Jiulongwan sections (intra-shelf basin) exhibit significantly low I/(Ca + Mg) ratios with a nadir lower than 0.1 μmol/mol, suggesting strongly anoxic conditions ($[O_2] < 1–3$ μM). In contrast, the Daotuo and Siduping sections (outer shelf–slope) show increased I/(Ca + Mg) ratios (up to 4.53 in the Daotuo and 1.29 in the Siduping) relative to the lower parts of the Doushantuo Formation (Fig. 5). Large negative C isotope excursions in this interval have been also proposed as a globally diagenetic event (e.g., Oehlert and Swart, 2014; Wei et al., 2022b). Variations of I/(Ca + Mg) ratios of the carbonates across the transection of the Yangtze area seem to be linked to diagenetic alteration. Large C isotope excursions corresponding to low I/(Ca + Mg) in the proximal sections and muted C isotope excursions corresponding to high I/(Ca + Mg) in the distal sections are consistent with more sediment-buffered conditions in the deeper sections that potentially preserve the primary geochemical signals (Hardisty et al., 2017; Wei et al., 2022a; Busch et al., 2022). Moreover, in step with the nadirs of negative C isotope excursion, Ce/Ce* of the carbonates are high (> 0.8) in the Jiulongwan section but notably decreased in the Daotuo and Siduping sections (lowest to 0.1) (also see Cheng et al., 2022), providing independent evidence for different redox landscapes in these sections. Regardless of diagenetic alteration, relatively higher I/(Ca + Mg) signals in the distal sections than those in the proximal and restricted regions may partly reflect the oxygenation of open ocean during the 'Shuram-Wonoka excursions' and the redox heterogeneity on the Yangtze margin (lower chemocline in more open oceans) (e.g., Wei et al., 2019). In this context, we suggest that 'Shuram-Wonoka excursions' along with other carbon isotope excursions in the late Neoproterozoic may be marked by pulsed consumption of oceanic reductants (e.g., dissolved organic carbon), instead of increased dissolved O_2 in the seawater (cf. Chen et al., 2022).

4.2.2. *The Dengying Formation in South China (ca. 551–541 Ma)*

In the late Ediacaran (ca. 551–541 Ma), shallow seawater of the intra-shelf basin on the Yangtze margin has been characterized by increased oxygenation levels, evidenced from gradually decreased Ce/Ce* (lowest to 0.3 in the uppermost Dengying Formation) in the Gaojiaxi-Yanjiahe section (Ling et al., 2013). However, new I/(Ca + Mg) data exhibit different or arguably opposed trends, compared to Ce/Ce*, in the Dengying Formation of the Gaojiaxi-Yanjiahe section (Fig. 3). All the Dengying carbonates in the Gaojiaxi-Yanjiahe section show notably low I/(Ca + Mg) values, decreasing from 0.25 to 0.12 throughout

(Fig. 3). By contrast, the Xiaotan section deposited on the inner-shelf platform show higher I/(Ca + Mg) ratios from 0.18 to 2.39 in the Dengying Formation, relative to the Gaojiaxi-Yanjiahe section deposited in the intrashelf basin. If diagenetic alterations dominated the I/(Ca + Mg) variations of the Dengying Formation, the shallower Xiaotan section should have documented lower I/(Ca + Mg) ratios than the deeper Gaojiaxi-Yanjiahe section as the fluid-buffered conditions more likely dominate in the shallower sites. The Dengying Formation in the Gaojiaxi-Yanjiahe section exhibits relatively low and uniform I/(Ca + Mg) ratios in both dolostone and limestone intervals. At this section, the Shibantan Member is proposed to experience the sediment-buffered conditions and more likely documents the primary geochemical signals relative to other members of the Dengying Formation (Wei et al., 2022a). Taken together, we suggest that redox stratification of the shallow seawater likely determines I/(Ca + Mg) ratios of carbonates in the Gaojiaxi-Yanjiahe and Xiaotan sections more than diagenetic alterations.

The I/(Ca + Mg) and Ce/Ce* signals appear to be decoupled in the Dengying Formation (i.e., high I/(Ca + Mg) and muted negative Ce anomaly in the Xiaotan section; low I/(Ca + Mg) and significant negative Ce anomaly in the Gaojiaxi-Yanjiahe section) (Fig. 3). The different behaviors in these two proxies may be attributed to the formation of particulate Mn (IV) that dominates the scavenging of Ce (IV) from the water column (Ling et al., 2013; Tostevin, 2021). In modern Black Sea (analogous to ancient redox stratified oceans, Fig. 2B), the nadir of seawater Ce/Ce* corresponds to the peak of particulate Mn (IV) in near anoxic seawater. If carbonates capture Ce/Ce* signal at this water depth, the lowest Ce/Ce* values do not actually record the highest dissolved O_2 concentrations at this depth, but represent highly oxygenated waters existing in the overlying water column (Ling et al., 2013). The decoupling between I/(Ca + Mg) and Ce/Ce* is likely related to the depth of oxycline vs. the depth of particulate Mn peak.

4.2.3. The Zhujiaqing Formation in the South China (ca. 541–525 Ma)

The Zhujiaqing Formation in the Xiaotan section documents large variations of I/(Ca + Mg) ratios ranging from near zero to 5.09 (Fig. 3). Overall, high I/(Ca + Mg) ratios are observed in the lower Cambrian Daibu and Zhongyicun members (ca. 541–531 Ma), indicative of increased dissolved O_2 concentrations, likely in phase with higher atmospheric oxygen levels (Wei et al., 2020). Relatively low Ce/Ce* values (lowest to 0.4) also support increased oxygen levels of shallow seawater in this interval (Fig. 3). In contrast, the Dahai Member (ca. 531–525 Ma) shows notably low I/(Ca + Mg) ratios (< 0.1 μmol/mol) and high Ce/Ce* values (> 0.6). The limestones in the Dahai Member are proposed to experience the sediment-buffered diagenesis that potentially preserve the primary geochemical signals (Wei et al., 2022a). Thus, the combination of low I/(Ca + Mg) and high Ce/Ce* more likely indicates rapid expansion of anoxic seawater on the Yangtze margin during the Cambrian Age 2, consistent with U isotope data (Wei et al., 2018).

4.3. The shallow-seawater redox dynamics from the Ediacaran to the early Cambrian (ca. 635–525 Ma)

To better contextualize the local/regional shallow seawater redox changes, we compile the I/(Ca + Mg) and U isotope ($\delta^{238}U$) data from the same carbonate successions (Fig. 7). Majority of I/(Ca + Mg) values of the early Ediacaran carbonates are below or around 0.5 μmol/mol with only several higher points, similar to the previously reported range for Precambrian carbonate baseline (Hardisty et al., 2014, 2017) but are significantly lower than those values from oxygenated sites during Mesozoic and Cenozoic (Lu et al., 2018). For modern seawater column in the OMZs (Fig. 2A), IO_3^- concentrations are strongly affected by the depth of anoxic water (referred to as oxycline) where IO_3^- reduction occurs in water column (e.g., Zhou et al., 2014; Hardisty et al., 2017). The most likely scenario for the low baseline I/(Ca + Mg) and muted negative Ce anomaly (Ce/Ce* > 0.8) is that the oxycline remained generally shallow throughout the early Ediacaran period. The shallow-water oxygenation level on continental margins (i.e., Yangtze marginal area in this study) appears to be lower than that of the modern ocean, consistent with extensive global seafloor anoxia during this interval based on $\delta^{238}U$ data (Fig. 7).

The middle to late Ediacaran (from the onset of 'Shuram-Wonoka excursion' in ca. 575 Ma) marks initial increases in I/(Ca + Mg) along with negative Ce anomaly (Fig. 7), indicative of effective accumulations of dissolved O_2 in very shallow seawater. Increase in shallow-water oxygenation levels also coincides with decreased global anoxic seafloor based on U isotope data (Zhang et al., 2019), indicating a potentially global contraction of OMZs. Nevertheless, large spatial variabilities in I/(Ca + Mg) suggest noticeable redox heterogeneity across the shelf-to-basin transects on the Yangtze margin (Li et al., 2020). The deeper waters in intrashelf basin during this period (e.g., Xiangerwan and Jiulongwan sections) are characterized by more reducing conditions relative to the early Ediacaran. In this view, the oxycline in the seawater column is greatly shallow and overall oxygen levels of the middle to late Ediacaran oceans are much lower than that of modern ocean (e.g., Sahoo et al., 2016).

The late Ediacaran–early Cambrian oceans (ca. 575–525 Ma) are characterized by large temporal fluctuations of shallow-water redox states, which is also consistent with U isotope records for global anoxic seafloor (Zhang et al., 2018; Wei et al., 2018). In the upper Ediacaran Dengying Formation in the Yangtze area (ca. 551–541 Ma), both the shallower Xiaotan section and deeper Yangtze Gorges sections show significantly low $\delta^{238}U$ values, indicative of extensive global oceanic anoxia. However, these two areas exhibit different trends in I/(Ca + Mg) ratios. Such observations suggest highly stratified seawater—increased oxygen levels of very shallow or surface seawater but persistent anoxic conditions in deeper seawater. The Dahai Member in the Xiaotan section documents uniformly high Ce/Ce*, low I/(Ca + Mg) and $\delta^{238}U$ values, suggesting consistently decreased oxygenation levels of both shallow and deep/pelagic seawater during the Cambrian Age 2 (Fig. 6). The expansion of O_2-depleted seawater on local and global scales in the Age 2 coincides with a notably large positive C isotope excursion (up to +8‰ on the Yangtze platform so called 'ZHUCE'). Despite the global or regional origin for this C isotope excursion, significant increases in marine primary productivity may have driven rapid consumption of dissolved O_2 in seawater, which results in shallowing oxycline and expansion of anoxic seawater. Although high primary productivity may lead to O_2 release to the atmosphere, the oxygenation of oceans can be highly delayed in the deep time when the atmospheric O_2 baseline is low (He et al., 2019; Reinhard and Planavsky, 2020; Wei et al., 2021b). Taken together, the Cambrian Age 2 is characterized by much lower oceanic oxygenation level compared to the late Ediacaran, during which anoxic conditions mark both shallow and global deep seawater.

4.4. Implications for Ediacaran–Cambrian metazoan radiations

New results of I/(Ca + Mg) and Ce/Ce* in this study provide considerable evidence for increases in shallow-water oxygen levels on continental margins that may have occurred at the onset of the 'Shuram-Wonoka Excursions' during the middle Ediacaran (< ca. 575 Ma) (Fig. 7C and D), which coincides with the rise of Ediacara biota (Xiao and Laflamme, 2009). Meanwhile, relatively low I/(Ca + Mg) ratios from the Ediacaran to the early Cambrian suggest that the overall dissolved O_2 concentrations of shallow seawater are much lower than those of well-oxygenated modern oceans (Fig. 7D) (Lu et al., 2018). No substantial rise of dissolved O_2 concentrations observed from the middle Ediacaran to the early Cambrian may suggest that the latest Ediacaran biomineralization is not solely driven by increased oxygenation levels (cf. Wood et al., 2017). Additionally, shallow seawater experiences rapid swings of dissolved O_2 concentrations from the middle Ediacaran to the early Cambrian (ca. 575–525 Ma) and shows strong spatial

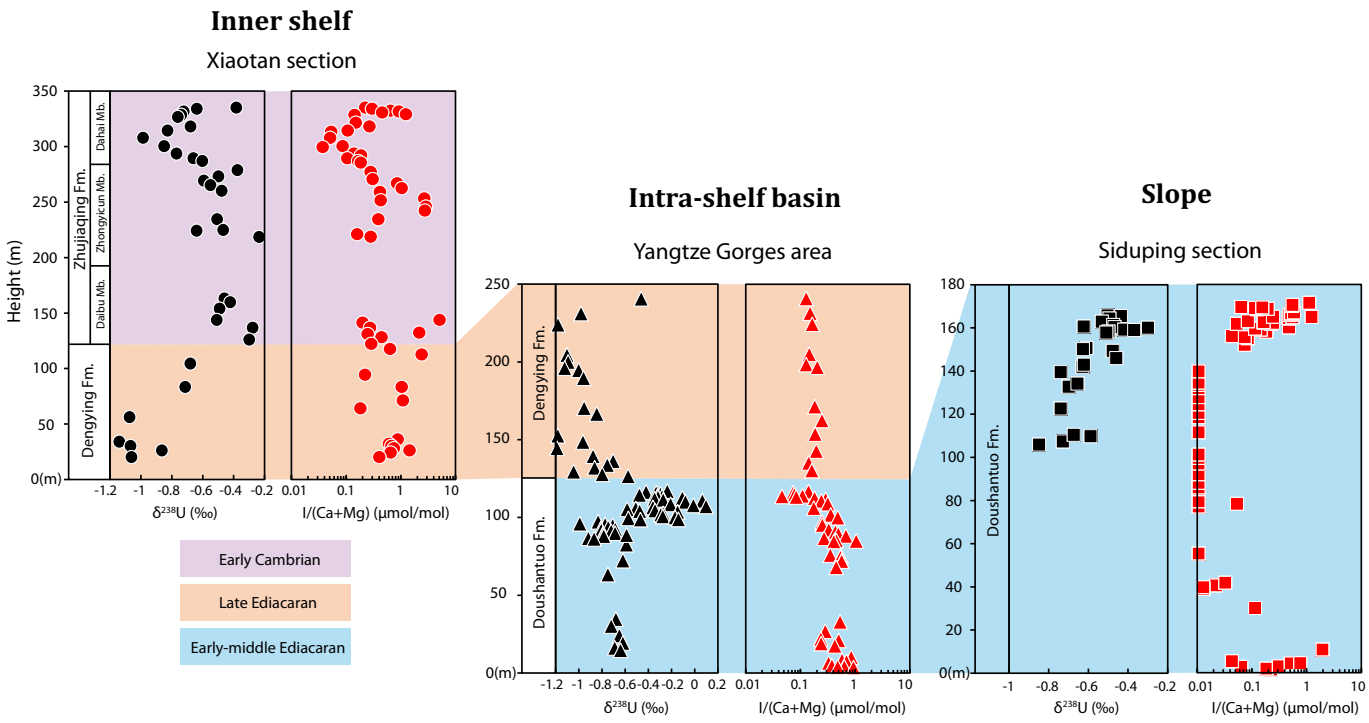

Fig. 6. Correlations of $\delta^{238}U$ and I/(Ca + Mg) data in the carbonates on the Yangtze margin, South China. The $\delta^{238}U$ data source: Xiaotan section (Wei et al., 2018); Yangtze Gorges are (Wei et al., 2018; Zhang et al., 2018, 2019); Siduping section (Cao et al., 2020).

heterogeneity (cf. Li et al., 2018). Particularly, the late Ediacaran to the Cambrian Age 2 (ca. 551–525 Ma) may have been marked by decreases in dissolved O_2 concentrations of shallow seawater (Fig. 7B). All the observations suggest that well-oxygenated shallow-water habitats are limited through the Ediacaran and the early Cambrian. There are no uniform stepwise increase in oxygenation levels in both shallow and global deep seawater on the eve of the proper Cambrian explosion (Fig. 7B, C, D). The key events of biological evolution (e.g., biomineralization, early metazoan innovation) may have occurred in spatially-temporally dynamic and hypoxic environment, rather than resiliently oxygenated seawater (Fig. 7).

Previous studies of global oceanic redox states (e.g., Mo and U isotopes) have suggested highly fluctuated and low oxygenation levels of global ocean from the Ediacaran to the Cambrian (see Wei et al., 2021a for a review). Habitat fragmentation and ecological reconstructing linked to global oceanic redox instability are proposed to facilitate the generation of evolutionary novelties and biological innovations during this interval. The I/(Ca + Mg) and Ce/Ce* data in this study highlight that, in addition to global deep ocean, shallow seawater on continental margins (e.g., the Yangtze margin)shows large spatiotemporal variabilities in dissolved O_2 concentrations, and average oxygenation levels of the early Cambrian oceans may not be much higher than those of middle-late Ediacaran oceans. Frequent development of O_2-deficient seawater in the habitats may provide an environmental barrier that affects biogeographic, ecological and evolutionary development of early metazoan communities (Tostevin et al., 2016; Hammarlund et al., 2017). However, since the early metazoans do not require as high oxygen levels as in modern ocean, the redox perturbations likely serve as a spur, rather than an impediment, to radiation and diversification of the metazoans (e.g., Wood and Erwin, 2018).

5. Conclusions

This study reports new I/(Ca + Mg) and Ce/Ce* data from two continuous carbonate successions, along with published data in South China to reconstruct the shallow-water redox landscapes from the Ediacaran to early Cambrian (ca. 635–525 Ma). Consistently low I/(Ca + Mg) ratios and high Ce/Ce* values of the carbonates indicate very limited oxygenation of shallow seawater on the Yangtze margin during the early–middle Ediacaran (ca. 635–575 Ma). The onset of shallow-water oxygenation may occur in the middle Ediacaran 'Shuram-Wonoka Excursions' (ca. < 575 Ma) with high redox heterogeneity on continental margins, which coincides with the rise of the Ediacara biota. The late Ediacaran to the early Cambrian shows frequent redox fluctuations of shallow seawater on the eve of the Cambrian explosion, during which average oxygenation levels are higher than those of the early Ediacaran but significantly lower than those of fully oxygenated ocean during the Phanerozoic. These observations suggest that the evolution of early metazoans may not require very high oxygen levels in their habitats as previously estimated. And the spatial and temporal redox instability of shallow seawater may have facilitated the diversification of early metazoans through enhancing habitat fragmentation, biological turnover and innovation.

CRediT authorship contribution statement

Guang-Yi Wei: Writing – review & editing, Writing – original draft, Validation, Resources, Methodology, Investigation, Data curation, Conceptualization. **Da Li:** Writing – review & editing, Validation, Resources, Methodology, Investigation, Formal analysis, Data curation. **Zunli Lu:** Writing – review & editing, Writing – original draft, Validation, Methodology, Investigation, Formal analysis, Data curation, Conceptualization. **Ganqing Jiang:** Writing – review & editing, Validation, Investigation, Data curation. **Hong-Fei Ling:** Writing – review & editing, Validation, Supervision, Resources, Methodology, Investigation, Funding acquisition.

Declaration of competing interest

The authors declare that they have no known competing financial interests or personal relationships that could have appeared to influence the work reported in this paper.

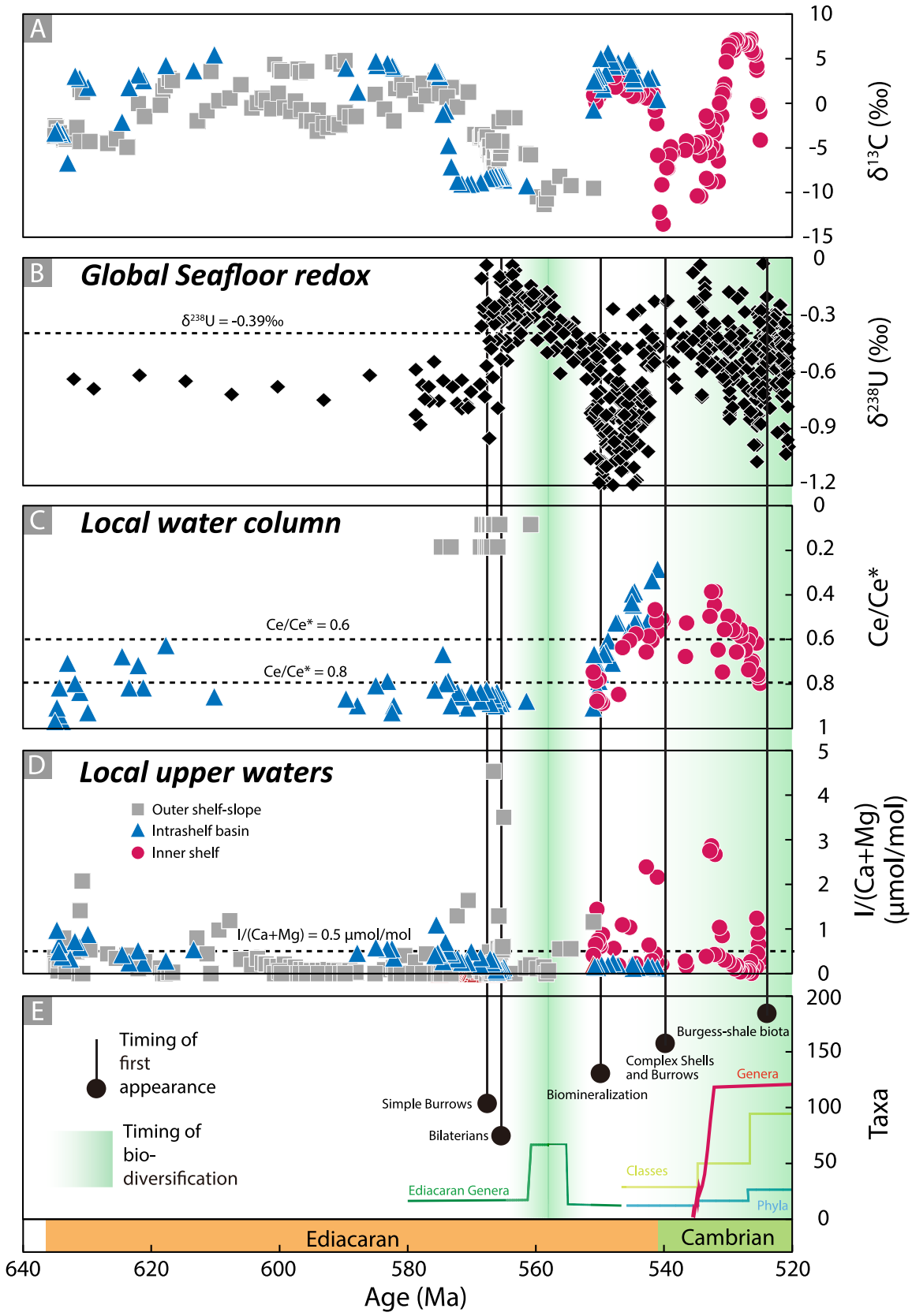

Fig. 7. Covariations of $\delta^{13}C$, Ce/Ce* and I/(Ca + Mg) data in carbonates, along with published $\delta^{238}U$ data (modified from Wei et al., 2021a) from the Ediacaran to early Cambrian (ca. 635–520 Ma) and their links with temporal occurrence ranges for key events of biological evolution (modified after Erwin et al., 2011; Wood et al., 2019). The dashed line in (B) represent the $\delta^{238}U$ value of modern seawater. The dashed lines in (C) denote potential thresholds for negative Ce anomalies. The dashed line in (D) represent the Precambrian I/(Ca + Mg) baseline (Hardisty et al., 2017; Lu et al., 2017).

Data availability

Data will be made available on request.

Acknowledgments

This study was funded by the National Natural Science Foundation of China (42373056, 41672026). Lu is supported by NSF EAR-2121445.

Appendix A. Supplementary data

Supplementary data to this article can be found online at https://doi.org/10.1016/j.gloplacha.2024.104522.

References

Ahm, A.-S.C., Bjerrum, C.J., Blättler, C.L., Swart, P.K., Higgins, J.A., 2018. Quantifying early marine diagenesis in shallow-water carbonate sediments. Geochim. Cosmochim. Acta 236, 140–159.
Bowyer, F.T., Zhuravlev, A.Y., Wood, R., Shields, G.A., Zhou, Y., Curtis, A., Poulton, S. W., Condon, D.J., Yang, C., Zhu, M., 2022. Calibrating the temporal and spatial dynamics of the Ediacaran - Cambrian radiation of animals. Earth Sci. Rev. 225, 103913.
Broecker, W., Peng, T., 1982. Tracers in the Sea. Lamont-Doherty Geological Observatory, Palisades, NY.
Busch, J.F., Hodgin, E.B., Ahm, A.-S.C., Husson, J.M., Macdonald, F.A., Bergmann, K.D., Higgins, J.A., Strauss, J.V., 2022. Global and local drivers of the Ediacaran Shuram carbon isotope excursion. Earth Planet. Sci. Lett. 579, 117368.
Butterfield, N.J., 2009. Oxygen, animals and oceanic ventilation: an alternative view. Geobiology 7, 1–7.
Byrne, R.H., Kim, K.-H., 1990. Rare earth element scavenging in seawater. Geochim. Cosmochim. Acta 54, 2645–2656.
Cao, M., Daines, S.J., Lenton, T.M., Cui, H., Algeo, T.J., Dahl, T.W., Shi, W., Chen, Z.-Q., Anbar, A., Zhou, Y.-Q., 2020. Comparison of Ediacaran platform and slope δ238U records in South China: Implications for global-ocean oxygenation and the origin of the Shuram Excursion. Geochim. Cosmochim. Acta 287, 111–124.
Chen, B., Hu, C., Mills, B.J.W., He, T., Andersen, M.B., Chen, X., Liu, P., Lu, M., Newton, R.J., Poulton, S.W., Shields, G.A., Zhu, M., 2022. A short-lived oxidation event during the early Ediacaran and delayed oxygenation of the Proterozoic Ocean. Earth Planet. Sci. Lett. 577, 117274.
Cheng, M., Wang, H., Li, C., Luo, G., Huang, J., She, Z., Lei, L., Ouyang, G., Zhang, Z., Dodd, M.S., Algeo, T.J., 2022. Barite in the Ediacaran Doushantuo Formation and its implications for marine carbon cycling during the largest negative carbon isotope excursion in Earth's history. Precambrian Res. 368.
Cole, D.B., Mills, D.B., Erwin, D.H., Sperling, E.A., Porter, S.M., Reinhard, C.T., Planavsky, N.J., 2020. On the co-evolution of surface oxygen levels and animals. Geobiology 18, 260–281.
Condon, D., Zhu, M., Bowring, S., Wang, W., Yang, A., Jin, Y., 2005. U-Pb ages from the neoproterozoic Doushantuo Formation, China. Science 308, 95–98.
Darroch, S.A.F., Smith, E.F., Laflamme, M., Erwin, D.H., 2018. Ediacaran extinction and cambrian explosion. Trends Ecol. Evol. 33, 653–663.
Erwin, D.H., Laflamme, M., Tweedt, S.M., Sperling, E.A., Pisani, D., Peterson, K.J., 2011. The Cambrian conundrum: early divergence and later ecological success in the early history of animals. Science 334, 1091–1097.
Hammarlund, E.U., Gaines, R.R., Prokopenko, M.G., Qi, C., Hou, X.-G., Canfield, D.E., 2017. Early Cambrian oxygen minimum zone-like conditions at Chengjiang. Earth Planet. Sci. Lett. 475, 160–168.
Hardisty, D.S., Lu, Z., Planavsky, N.J., Bekker, A., Philippot, P., Zhou, X., Lyons, T.W., 2014. An iodine record of Paleoproterozoic surface ocean oxygenation. Geology 42, 619–622.
Hardisty, D.S., Lu, Z., Bekker, A., Diamond, C.W., Gill, B.C., Jiang, G., Kah, L.C., Knoll, A. H., Loyd, S.J., Osburn, M.R., Planavsky, N.J., Wang, C., Zhou, X., Lyons, T.W., 2017. Perspectives on Proterozoic surface ocean redox from iodine contents in ancient and recent carbonate. Earth Planet. Sci. Lett. 463, 159–170.
Hardisty, D.S., Horner, T.J., Evans, N., Moriyasu, R., Babbin, A.R., Wankel, S.D., Moffett, J.W., Nielsen, S.G., 2021. Limited iodate reduction in shipboard seawater incubations from the Eastern Tropical North Pacific oxygen deficient zone. Earth Planet. Sci. Lett. 554.
He, T., Zhu, M., Mills, B.J.W., Wynn, P.M., Zhuravlev, A.Y., Tostevin, R., Pogge von Strandmann, P.A.E., Yang, A., Poulton, S.W., Shields, G.A., 2019. Possible links between extreme oxygen perturbations and the Cambrian radiation of animals. Nat. Geosci. 12, 468–474.
He, R., Jiang, G., Lu, W., Lu, Z., 2020. Iodine records from the Ediacaran Doushantuo cap carbonates of the Yangtze Block, South China. Precambrian Res. 347, 105843.
Higgins, J.A., Blättler, C.L., Lundstrom, E.A., Santiago-Ramos, D.P., Akhtar, A.A., Crüger Ahm, A.S., Bialik, O., Holmden, C., Bradbury, H., Murray, S.T., Swart, P.K., 2018. Mineralogy, early marine diagenesis, and the chemistry of shallow-water carbonate sediments. Geochim. Cosmochim. Acta 220, 512–534.
Jiang, G., Shi, X., Zhang, S., Wang, Y., Xiao, S., 2011. Stratigraphy and paleogeography of the Ediacaran Doushantuo Formation (ca. 635–551Ma) in South China. Gondwana Res. 19, 831–849.
Kerisit, S.N., Smith, F.N., Saslow, S.A., Hoover, M.E., Lawter, A.R., Qafoku, N.P., 2018. Incorporation Modes of Iodate in Calcite. Environ. Sci. Technol. 52, 5902–5910.
Lawrence, M.G., Greig, A., Collerson, K.D., Kamber, B.S., 2006. Rare Earth Element and Yttrium Variability in South East Queensland Waterways. Aquat. Geochem. 12, 39–72.
Lenton, T.M., Boyle, R.A., Poulton, S.W., Shields-Zhou, G.A., Butterfield, N.J., 2014. Co-evolution of eukaryotes and ocean oxygenation in the Neoproterozoic era. Nat. Geosci. 7, 257–265.
Li, G., Xiao, S., 2004. Tannuolina and Micrina (Tannuolinidae) from the Lower Cambrian of eastern Yunnan, South China, and their scleritome reconstruction. J. Paleontol. 78, 900–913.
Li, D., Ling, H.-F., Shields-Zhou, G.A., Chen, X., Cremonese, L., Och, L., Thirlwall, M., Manning, C.J., 2013. Carbon and strontium isotope evolution of seawater across the Ediacaran–Cambrian transition: Evidence from the Xiaotan section, NE Yunnan, South China. Precambrian Res. 225, 128–147.
Li, C., Cheng, M., Zhu, M., Lyons, T.W., 2018. Heterogeneous and dynamic marine shelf oxygenation and coupled early animal evolution. Emerg. Top. Life Sci. 2, 279–288.
Li, C., Shi, W., Cheng, M., Jin, C., Algeo, T.J., 2020. The redox structure of Ediacaran and early Cambrian oceans and its controls. Sci. Bull. 65, 2141–2149.
Ling, H.-F., Chen, X., Li, D., Wang, D., Shields-Zhou, G.A., Zhu, M., 2013. Cerium anomaly variations in Ediacaran–earliest Cambrian carbonates from the Yangtze Gorges area, South China: Implications for oxygenation of coeval shallow seawater. Precambrian Res. 225, 110–127.
Liu, X.-M., Hardisty, D.S., Lyons, T.W., Swart, P.K., 2019. Evaluating the fidelity of the cerium paleoredox tracer during variable carbonate diagenesis on the Great Bahamas Bank. Geochim. Cosmochim. Acta 248, 25–42.
Lu, Z., Jenkyns, H.C., Rickaby, R.E.M., 2010. Iodine to calcium ratios in marine carbonate as a paleo-redox proxy during oceanic anoxic events. Geology 38, 1107–1110.
Lu, Z., Hoogakker, B.A.A., Hillenbrand, C.-D., Zhou, X., Thomas, E., Gutchess, K.M., Lu, W., Jones, L., Rickaby, R.E.M., 2016. Oxygen depletion recorded in upper waters of the glacial Southern Ocean. Nat. Commun. 7, 11146.
Lu, W., Wörndle, S., Halverson, G.P., Zhou, X., Bekker, A., Rainbird, R.H., Hardisty, D.S., Lyons, T.W., Lu, Z., 2017. Iodine proxy evidence for increased ocean oxygenation during the Bitter Springs Anomaly. Geochem. Perspect. Lett. 5, 53–57.
Lu, W., Ridgwell, A., Thomas, E., Hardisty, D.S., Luo, G., Algeo, T.J., Saltzman, M.R., Gill, B.C., Shen, Y., Ling, H.F., Edwards, C.T., Whalen, M.T., Zhou, X., Gutchess, K. M., Jin, L., Rickaby, R.E.M., Jenkyns, H.C., Lyons, T.W., Lenton, T.M., Kump, L.R., Lu, Z., 2018. Late inception of a resiliently oxygenated upper ocean. Science 361, 174–177.
Lu, Z., Lu, W., Rickaby, R.E.M., Thomas, E., 2020. Earth history of oxygen and the iprOxy. In: Lyons, T., Turchyn, A., Reinhard, C. (Eds.), Geochemical Tracers in Earth System Science. Cambridge University Press.
Lyons, T.W., Reinhard, C.T., Planavsky, N.J., 2014. The rise of oxygen in Earth's early ocean and atmosphere. Nature 506, 307–315.
Marshall, C.R., 2006. Explaining the Cambrian "Explosion" of animals. Annu. Rev. Earth Planet. Sci. 34, 355–384.
McFadden, K.A., Huang, J., Chu, X., Jiang, G., Kaufman, A.J., Zhou, C., Yuan, X., Xiao, S., 2008. Pulsed oxidation and biological evolution in the Ediacaran Doushantuo Formation. Proc. Nat. Acad. Sci. USA 105, 3197–3202.
Mills, D.B., Ward, L.M., Jones, C., Sweeten, B., Forth, M., Treusch, A.H., Canfield, D.E., 2014. Oxygen requirements of the earliest animals. Proc. Nat. Acad. Sci. USA 111, 4168–4172.
Och, L.M., Shields-Zhou, G.A., 2012. The Neoproterozoic oxygenation event: Environmental perturbations and biogeochemical cycling. Earth Sci. Rev. 110, 26–57.
Oehlert, A.M., Swart, P.K., 2014. Interpreting carbonate and organic carbon isotope covariance in the sedimentary record. Nat. Commun. 5, 4672.
Pourmand, A., Dauphas, N., Ireland, T.J., 2012. A novel extraction chromatography and MC-ICP-MS technique for rapid analysis of REE, Sc and Y: revising CI-chondrite and Post-Archean Australian Shale (PAAS) abundances. Chem. Geol. 291, 38–54.
Reinhard, C.T., Planavsky, N.J., 2020. Biogeochemical controls on the redox evolution of Earth's oceans and atmosphere. Elements 16, 191–196.
Reinhard, C.T., Planavsky, N.J., Olson, S.L., Lyons, T.W., Erwin, D.H., 2016. Earth's oxygen cycle and the evolution of animal life. Proc. Nat. Acad. Sci. USA 113, 8933–8938.
Rooney, A.D., Cantine, M.D., Bergmann, K.D., Gomez-Perez, I., Al Baloushi, B., Boag, T. H., Busch, J.F., Sperling, E.A., Strauss, J.V., 2020. Calibrating the coevolution of Ediacaran life and environment. Proc. Natl. Acad. Sci. USA 117, 16824–16830.
Rue, E.L., Smith, G.J., Cutter, G.A., Bruland, K.W., 1997. The response of trace element redox couples to suboxic conditions in the water column. Deep-Sea Res., Part 1: Oceanogr. Res. Pap. 44, 113–134.
Sahoo, S.K., Planavsky, N.J., Jiang, G., Kendall, B., Owens, J.D., Wang, X., Shi, X., Anbar, A.D., Lyons, T.W., 2016. Oceanic oxygenation events in the anoxic Ediacaran Ocean. Geobiology 14, 457–468.
Servais, T., Harper, D.A.T., 2018. The Great Ordovician Biodiversification Event (GOBE): definition, concept and duration. Lethaia 51, 151–164.
Shang, M., Tang, D., Shi, X., Zhou, L., Zhou, X., Song, H., Jiang, G., 2019. A pulse of oxygen increase in the early Mesoproterozoic Ocean at ca. 1.57–1.56 Ga. Earth Planet. Sci. Lett. 527, 115797.
Sholkovitz, E., Shen, G.T., 1995. The incorporation of rare earth elements in modern coral. Geochim. Cosmochim. Acta 59, 2749–2756.
Sperling, E.A., Frieder, C.A., Raman, A.V., Girguis, P.R., Levin, L.A., Knoll, A.H., 2013. Oxygen, ecology, and the Cambrian radiation of animals. Proc. Nat. Acad. Sci. USA 110, 13446–13451.

Sperling, E.A., Knoll, A.H., Girguis, P.R., 2015a. The Ecological Physiology of Earth's Second Oxygen Revolution. Annu. Rev. Ecol. Evol. Syst. 46, 215–235.
Sperling, E.A., Wolock, C.J., Morgan, A.S., Gill, B.C., Kunzmann, M., Halverson, G.P., Macdonald, F.A., Knoll, A.H., Johnston, D.T., 2015b. Statistical analysis of iron geochemical data suggests limited late Proterozoic oxygenation. Nature 523, 451–454.
Stolper, D.A., Keller, C.B., 2018. A record of deep-ocean dissolved O_2 from the oxidation state of iron in submarine basalts. Nature 553, 323–327.
Tarhan, L.G., Droser, M.L., Cole, D.B., Gehling, J.G., 2018. Ecological expansion and extinction in the late Ediacaran: weighing the evidence for environmental and biotic drivers. Integr. Comp. Biol. 58, 688–702.
Tostevin, R., 2021. Cerium anomalies and paleoredox. In: Lyons, T., Turchyn, A., Reinhard, C. (Eds.), Geochemical Tracers in Earth System Science. Cambridge University Press.
Tostevin, R., Mills, B.J.W., 2020. Reconciling proxy records and models of Earth's oxygenation during the Neoproterozoic and Palaeozoic. Interface Focus 10, 20190137.
Tostevin, R., Wood, R.A., Shields, G.A., Poulton, S.W., Guilbaud, R., Bowyer, F., Penny, A.M., He, T., Curtis, A., Hoffmann, K.H., Clarkson, M.O., 2016. Low-oxygen waters limited habitable space for early animals. Nat. Commun. 7, 12818.
Webb, G.E., Nothdurft, L.D., Kamber, B.S., Kloprogge, J.T., Zhao, J.-X., 2009. Rare earth element geochemistry of scleractinian coral skeleton during meteoric diagenesis: a sequence through neomorphism of aragonite to calcite. Sedimentology 56, 1433–1463.
Wei, G.-Y., Planavsky, N.J., Tarhan, L.G., Chen, X., Wei, W., Li, D., Ling, H.-F., 2018. Marine redox fluctuation as a potential trigger for the Cambrian explosion. Geology 46, 587–590.
Wei, H., Wang, X., Shi, X., Jiang, G., Tang, D., Wang, L., An, Z., 2019. Iodine content of the carbonates from the Doushantuo Formation and shallow ocean redox change on the Ediacaran Yangtze Platform, South China. Precambrian Res. 322, 160–169.
Wei, W., Frei, R., Gilleaudeau, G.J., Li, D., Wei, G.-Y., Huang, F., Ling, H.-F., 2020. Variations of redox conditions in the atmosphere and Yangtze Platform during the Ediacaran-Cambrian transition: Constraints from Cr isotopes and Ce anomalies. Palaeogeogr. Palaeoclimatol. Palaeoecol. 543, 109598.
Wei, G.-Y., Ling, H.-F., Shields, G.A., Hohl, S.V., Yang, T., Lin, Y.-B., Zhang, F., 2021a. Revisiting stepwise ocean oxygenation with authigenic barium enrichments in marine mudrocks. Geology 49, 1059–1063.
Wei, G.-Y., Planavsky, N.J., He, T., Zhang, F., Stockey, R., Cole, D.B., Lin, Y.-B., Ling, H.-F., 2021b. Global marine redox evolution from the late Neoproterozoic to the early Paleozoic constrained by the integration of Mo and U isotope records. Earth Sci. Rev. 214, 103506.
Wei, G.Y., Hood, A.V.S., Planavsky, N.J., Li, D., Ling, H.F., Tarhan, L.G., 2022a. Calcium isotopic constraints on the transition from aragonite seas to Calcite Seas in the Cambrian. Glob. Biogeochem. Cycles 36, e2021GB007235.
Wei, G.-Y., Wang, J., Planavsky, N.J., Zhao, M., Bolton, E.W., Jiang, L., Asael, D., Wei, W., Ling, H.-F., 2022b. On the origin of Shuram carbon isotope excursion in South China and its implication for Ediacaran atmospheric oxygen levels. Precambrian Res. 375, 106673.
Wong, G.T.F., 1991. The marine geochemistry of iodine. Rev. Aquat. Sci. 4, 45–73.
Wood, R., Erwin, D.H., 2018. Innovation not recovery: dynamic redox promotes metazoan radiations. Biol. Rev. 93, 863–873.
Wood, R., Ivantsov, A.Y., Zhuravlev, A.Y., 2017. First macrobiota biomineralization was environmentally triggered. Proc. Biol. Sci. 284, 20170059.
Wood, R., Liu, A.G., Bowyer, F., Wilby, P.R., Dunn, F.S., Kenchington, C.G., Cuthill, J.F. H., Mitchell, E.G., Penny, A., 2019. Integrated records of environmental change and evolution challenge the Cambrian Explosion. Nat. Ecol. Evol. 3, 528–538.
Xiao, S., Laflamme, M., 2009. On the eve of animal radiation: phylogeny, ecology and evolution of the Ediacara biota. Trends Ecol. Evol. 24, 31–40.
Yang, C., Rooney, A.D., Condon, D.J., Li, X.H., Grazhdankin, D.V., Bowyer, F.T., Hu, C., Macdonald, F.A., Zhu, M., 2021. The tempo of Ediacaran evolution. Sci. Adv. 7, eabi9643.
Zhang, X., Shu, D., Han, J., Zhang, Z., Liu, J., Fu, D., 2014. Triggers for the Cambrian explosion: Hypotheses and problems. Gondwana Res. 25, 896–909.
Zhang, F., Xiao, S., Kendall, B., Romaniello, S.J., Cui, H., Meyer, M., Gilleaudeau, G.J., Kaufman, A.J., Anbar, A.D., 2018. Extensive marine anoxia during the terminal Ediacaran Period. Sci. Adv. 4, eaan8983.
Zhang, F., Xiao, S., Romaniello, S.J., Hardisty, D., Li, C., Melezhik, V., Pokrovsky, B., Cheng, M., Shi, W., Lenton, T.M., Anbar, A.D., 2019. Global marine redox changes drove the rise and fall of the Ediacara biota. Geobiology 17, 594–610.
Zhou, X., Thomas, E., Rickaby, R.E.M., Winguth, A.M.E., Lu, Z., 2014. I/Ca evidence for upper ocean deoxygenation during the PETM. Paleoceanography 29, 964–975.